Article ID: 1006-8775(2009) 01-0162-05

INSTABILITY OF SYMMETRIC TYPHOON CIRCULATION AND ADAPTIVE OBSERVATION

GAO Shou-ting (高守亭)[1], ZHOU Fei-fan (周菲凡)[1], LIU Li-ping (刘黎平)[2]

(1. Laboratory of Cloud-Precipitation Physics and Severe Storms, Institute of Atmospheric Physics, Chinese Academy of Sciences, Beijing 100029 China; 2. State Key Laboratory of Severe Weather, Chinese Academy of Meteorological Sciences, Beijing 100081 China)

Abstract: This study presents a new way to identify the sensitive areas, which are determined by invoking the negative anomalies of moist potential vorticity (MPV) for typhoon adaptive observations. It is found that the areas of negative MPV are the symmetric instability areas and can be taken as sensitive areas for typhoon adaptive observations. Three typhoons in 2008, Nuri, Fung-wong, and Fengshen, were simulated with the help of MM5 model. It is shown that these typhoons are well simulated in the first 12 hours. Based on these investigations, the calculations of MPV are carried out sequentially. The result shows that the negative maxima of MPV are always around the typhoon eyes for all the cases, which means that the sensitive areas are also near them all the time.

Key words: typhoon; moist potential vorticity (MPV); instability; sensitive areas

CLC number: P433 **Document code:** A **doi:** 10.3969/j.issn.1006-8775.2009.02.005

1 INTRODUCTION

Studies have shown that, in a perfect model hypothesis, forecast errors are mainly caused by the initial analysis errors because of the scarce observation data and the immature data assimilation scheme [1-3]. Thus, supplementing observation in some areas lacking observational data is a main method to improve forecast. However, it is costly and unnecessary to add observations everywhere, especially for typhoon prediction, as the typhoons are almost all over the ocean during their lifetime, and it is shown that extensive observations obtained in the general region around the cyclones did not conclusively improve forecasts much more than observations only obtained in some particular regions [4, 5]. This is the idea of adaptive observation, and the particular regions are called sensitive areas [6, 7].

Obviously, the key point of adaptive observation is the determination of the sensitive area. Currently, there are some strategies for identifying the sensitive areas. One strategy is based on the adjoint technique, such as singular vectors (SVs) [8], adjoint sensitivities [9], and adjoint-derived sensitivity steering vector (ADSSV) [10]. These kinds of methods are also named adjoint-based sensitivities [11]. Another strategy is ensemble-based, such as the ensemble transform [12], the ensemble Kalman filter [13], and the ensemble transform Kalman filter [14]. In the mean time, other methodologies are also proposed in the sensitive area determination like the quasi-inverse linear method [15], and the breeding-like method mentioned in the study of Lorenz and Emanuel [16]. Recently, Mu et al. [17] applied the method of conditional nonlinear optimal perturbation (CNOP) to the sensitive-area identification for typhoon prediction, and the results showed that this method is promising. In a work of the application of CNOP to adaptive observations, Zhou [18] found that the CNOP-identified sensitive areas are always located at the unstable area of the background fields, with a part of the sensitive areas located around the eye in the strong convective region.

The above methodologies come from the dynamical viewpoints, and their identified sensitive areas are usually the place where the small initial errors would result in large forecast errors. In other

Received date: 2009-03-28; **revised date:** 2009-07-30

Foundation item: State Key Development Program for Basic Research of China (2009CB421505); Meteorological Special Project of The Ministry of Sciences and Technology of the People's Republic of China (GYHY200706020); Project of the Natural Science Foundation of China (40775031); Project of NO.2008 LASW-A01

Biography: GAO Shou-ting, PhD, undertaking the research on dynamic meteorology.

E-mail for correspondence author: gst@lasg.iap.ac.cn

words, the basic states in the sensitive area are usually unstable, as indicated by Zhou [18], Ehrendorfer and Errico [19], etc. Thus, it is thought that the identification of the sensitive area can be taken as the identification of the unstable area from the view of physics; thereby we can determine the sensitive areas by analyzing the atmospheric instability.

The stability can be classified into three types according to different forcing condition[20], such as the static stability when the vertical forcing is considered, the inertial stability when the horizontal forcing is considered, and the symmetric stability when both the vertical and horizontal forcing are considered. As for typhoons, there is strong slantwise ascending motion around the eye, and both the vertical and horizontal forcing exists. Thus the symmetric stability can be used to deal with the situation of typhoons.

Usually, when a typhoon is about to land, it is mature enough to be taken as axisymmetric. In this paper, therefore, we consider the instability of axisymmetric typhoon circulation to find the unstable areas for typhoons.

The structure of this paper is as follows. Section 2 provides a description of the methodology. Section 3 introduces the application of the methodology to three typhoon cases. Section 4 gives a brief summary and discussion.

2 METHODOLOGY

In this part, we will introduce the methodology from the viewpoints of energy and moist potential vorticity (MPV) respectively.

2.1 *The energy viewpoint*

In a cylindrical coordinate, the kinetic energy K can be written as

$$K = K_m + K_\varphi \tag{1}$$

where

$$K_m = \int \frac{1}{2}\rho\left(v_r^2 + v_z^2\right)dV, \tag{2}$$

$$K_\varphi = \int \frac{1}{2}\rho v_\varphi^2 dV = \int \rho \frac{M^2}{2r^2}dV = \int \rho M^2 R dV. \tag{3}$$

Here, M is an angular momentum equaling to $v_\varphi r$; v_r, v_z, v_φ are velocities in the r, z, φ directions respectively, ρ is the density, r is the radius, V is the volume, and $R = \frac{1}{2r^2}$. The internal energy U can be written as

$$U = \int \rho u dV \tag{4}$$

where u is the internal energy per mass.

The potential energy G is

$$G = \int \rho \Phi dV \tag{5}$$

where Φ is the potential energy per mass.

According to total energy conservation law, there is

$$E = K_m + J = const \tag{6}$$

where

$$J = K_\varphi + U + G = \int \rho(m^2 R + u + \Phi)dV. \tag{7}$$

Since

$$K_m \geq 0, \tag{8}$$

at the point where the energy E is the largest, there are

$$\begin{cases} \delta J = 0 \\ \delta^2 J < 0 \end{cases}. \tag{9}$$

It can result in

$$Qm\frac{\partial \Phi}{\partial z} < 0 \tag{10}$$

where Q is the potential vorticity (PV).

Inequality (10) is also the necessary condition of instability.

Because in the Northern Hemisphere there is

$$m\frac{\partial \Phi}{\partial z} > 0, \tag{11}$$

the necessary condition of instability is

$$Q < 0. \tag{12}$$

2.2 *The MPV viewpoint*

Dry potential vorticity may not contain important information as there is abundant water vapor in typhoons, the MPV is taken into account sequentially.

In a cylindrical coordinate, the MPV can be written as

$$Q_e = \frac{1}{\rho}\omega \cdot \nabla \theta_e = \frac{1}{\rho}\left(\omega_r \frac{\partial \theta_e}{\partial r} + \omega_z \frac{\partial \theta_e}{\partial z}\right) \tag{13}$$

where ω is the absolute vorticity, and θ_e is the potential temperature. ω_r, ω_z are the components of ω in the r, z directions respectively, and their expressions are as follows:

$$\omega_r = -\frac{1}{r}\frac{\partial m}{\partial z}, \tag{14}$$

$$\omega_z = \frac{1}{r}\frac{\partial m}{\partial r}. \tag{15}$$

Thus Eq. (13) can be written as

$$Q_e = \frac{1}{\rho r}\left(\frac{\partial m}{\partial r}\frac{\partial \theta_e}{\partial z} - \frac{\partial m}{\partial z}\frac{\partial \theta_e}{\partial r}\right). \tag{16}$$

Eq. (16) can be further expanded as follows:

$$Q_e = \frac{1}{\rho r}\frac{\partial m}{\partial z}\frac{\partial \theta_e}{\partial z}\left(\frac{\partial m}{\partial r}\Big/\frac{\partial m}{\partial z}\Big|_m - \frac{\partial \theta}{\partial r}\Big/\frac{\partial \theta_e}{\partial z}\Big|_{\theta_e}\right) \quad (17)$$

where $\frac{\partial m}{\partial r}\Big/\frac{\partial m}{\partial z}\Big|_m$ is the iso-angular momentum surface slope, and $\frac{\partial \theta_e}{\partial r}\Big/\frac{\partial \theta_e}{\partial z}\Big|_{\theta_e}$ is the isentrophic surface slope.

According to the theory of symmetric stability, when iso-angular momentum surface slope is smaller than the isentrophic surface slope, the symmetric instability happens. That is, the symmetric instability requires

$$\frac{\partial m}{\partial r}\Big/\frac{\partial m}{\partial z}\Big|_m < \frac{\partial \theta_e}{\partial r}\Big/\frac{\partial \theta_e}{\partial z}\Big|_{\theta_e}. \quad (18)$$

Namely, $Q_e < 0$, according to Eq. (17).

Figure 1 is the schematic diagram of symmetric instability.

Thus, we try to find the area where $Q_e < 0$ and identify it as a sensitive area for typhoons.

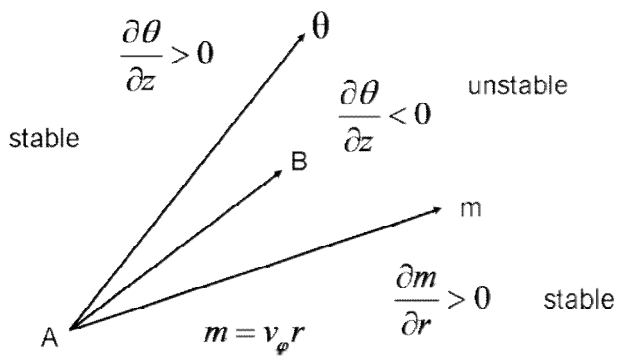

Fig.1 Schematic diagram of symmetric instability.

3 APPLICATION

3.1 *Experimental design*

The landing of a typhoon is the target and additional observations are added to improve the 24-hour forecast. That is, the observations will be supplemented 24 hours before the typhoon landing. Apparently, the observed position should be determined before implementation, and we assume that the decision is made 12 hours ahead, i.e., 36 hours before the landfall of the typhoon.

As mentioned above, for every typhoon case, we choose a 36-hour period to study. In this paper, three typhoon cases named Nuri, Fung-wong, and Fengshen occurring in 2008 are studied. These typhoons landed in the mainland of China, specifically, Nuri and Fengshen landed in Guangdong province, and Fung-wong landed in Fujian province, and the time periods leading up to their landing are studied. For the Nuri case, the time period is chosen from 0000 UTC 21 August to 1200 UTC 22 August, and the observations are to be added at 1200 UTC 21 August. For Fung-wong, the time period from 0000 UTC 27 July to 1200 UTC 28 July is chosen, with 1200 UTC 27 July being the observation time. The time period from 1200 UTC 23 June to 0000 UTC 25 June is chosen for the Fengshen case, and the observation time is 0000 UTC 24 June.

We use the model of the fifth generation Pennsylvania State University–National Center for Atmospheric Research (PSU-NCAR) Mesoscale Model (MM5; Dudhia[20]) to study these typhoons. For all cases, the resolution is 30 km and the vertical direction has been evenly divided into 20 sigma levels. The horizontal grids are 87×91 (latitude by longitude) for both Nuri and Fengshen cases, while 91×91 (latitude by longitude) for the Fung-wong case. The initial and boundary conditions are acquired from the National Centers for Environment Predictions (NCEP) Global Forecasting Systems (GFS) global analysis (1°×1°), with GFS boundary conditions supplied every 6 h during model integration. The physical parameterizations include the Kuo cumulus parameterization scheme, the Blackadar PBL scheme, the simple cooling radiation scheme, and the stable precipitation.

The MICAPS (Meteorological Information Combine Analysis and Process System) data are used to offer the observed typhoon tracks.

3.2 *Results*

Figure 2 presents the simulation tracks and the observation tracks for each case. It is shown that for these typhoons the first 12-hour simulations are better than the second 24-hour simulations, as the track prediction errors are less than 100 km in the first 12 hours. For the Fung-wong case, the simulation in the second 24 hours is also acceptable (Fig. 3b), as the track forecast errors are within 200 km. For the other two cases, especially for Fengshen case, the second 24 hours forecast errors are large (Fig. 3a & 3c). It can be seen that the typhoons of Nuri and Fengshen are predicted to move northeastward in the second 12 hours, which is obviously deviated from the observed tracks which depict the northwestward movement of the typhoons.

As mentioned in section 3, what we targeted in adaptive observation is the place where the

observations should be deployed 12 hours later, thus if the typhoon tracks can be better simulated in the first 12 hours, i.e., the simulation fields can be taken as the real situations for the first coming 12 hours, then we can determine the unstable areas according to the simulation results, since the real analysis cannot be obtained at the initial time.

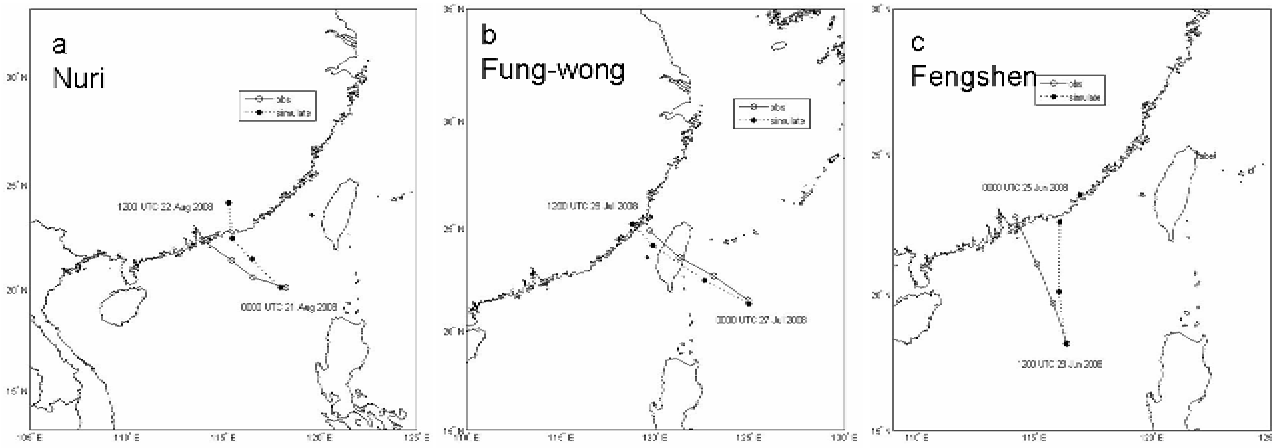

Fig.2 Simulation tracks (dashed) from nonlinear MM5 and observation tracks (solid) from CMA. (a) Nuri, from 0000 UTC 21 Aug to 1200 UTC 22 Aug 2008; (b) Fung-wong, from 0000 UTC 27 July to 1200 UTC 28 July 2008; (c) Fengshen, from 1200 UTC 23 June to 0000 UTC 25 June 2008.

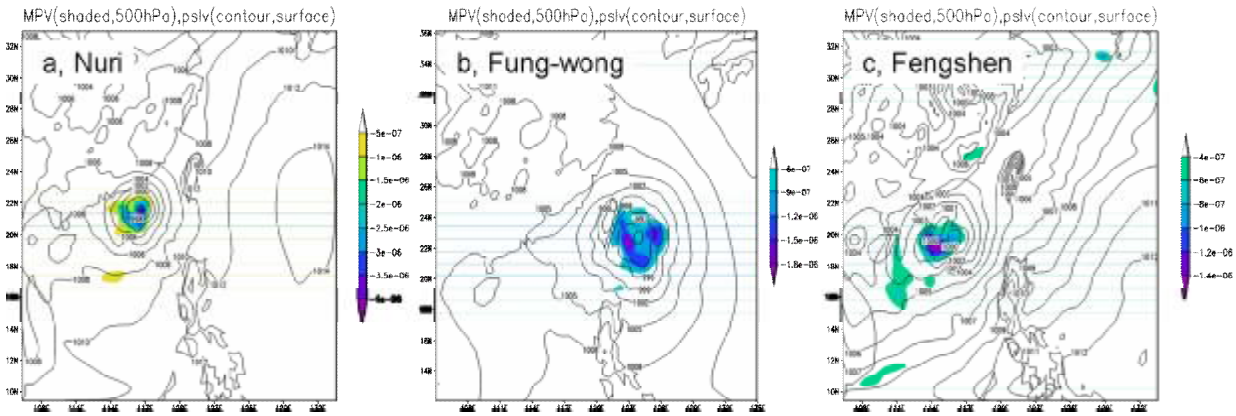

Fig.3 Distributions of negative MPV [shaded, unit: m2 · K/(s · kg)] on 500 hPa and the sea surface pressures (contour, unit: hPa) for (a)Nuri, (b)Fung-wong, and (c)Fengshen at the time of adding observations.

From Fig. 2, it is known that the typhoons are well simulated in the first 12 hours. Based on these simulations, we calculate the MPV. With the help of the methodology described in section 2, the atmosphere is unstable where the MPV is negative. Figure 3 indicates the distribution of MPV on 500 hPa at the time of adding observation. It is shown that the negative maximum of MPV is around or in the typhoon eye for these cases. For Nuri, the most unstable area is at the south edge of the typhoon eye; for Fung-wong, it is at the east and west edge; for Fengshen, it is at the southwest edge. These unstable areas are identified as the sensitive areas for each of the typhoons as mentioned in the introduction.

The distributions of the sensitive areas are of physical meanings, as it is known that there is strong convection around the typhoon eye, which may result in great instability. Although these locations may not be favorable for the adding of observations, they are indicated by the physical means.

4 SUMMARY AND DISCUSSION

In this paper, by combining the moist potential vorticity (MPV) theory and the symmetric instability, we found that the symmetric unstable areas are where the MPV is negative. Studies have revealed that the sensitive areas which are identified by using such dynamical methods as SV(singular vector) and CNOP (conditional nonlinear optimal perturbation) turn out to be unstable areas from the viewpoint of physics in

adaptive observations for improving typhoon predictions. Consequently, we identify the sensitive areas by analyzing the unstable areas of typhoons using MPV.

Three typhoon cases of Nuri, Fung-wong, and Fengshen occurring in 2008 have been studied. Results showed that these typhoons can be well simulated in the first 12 hours so that the MPV can be calculated based on the simulation results. For all the cases, the areas of negative MPV, or the unstable areas, are always located around the typhoon eye while the most unstable areas are a little different. This means that from the perspective of symmetric instability, the sensitive areas are always near the typhoon eye.

This is a primary study of the application of the symmetric instability in identifying the typhoon sensitive areas for adaptive observation. More studies should be done in future work. First, more typhoon cases should be studied. Second, it should be tested if the identified sensitive areas really help improve the prediction of typhoons. Third, the sensitive areas, determined by the theory of symmetric instability, should be compared with other sensitive areas identified by dynamical methods, and the difference should be further studied.

Nonetheless, this paper provides a new method to identify the sensitive areas in typhoon adaptive observations.

REFERENCES:

[1] RIEHL H, HAGGARD W H, SANBORN R W. On the prediction of 24-hour hurricane motion [J]. J. Meteor., 1956, 13: 415-420.

[2] SIMMONS A J, MEREAU R, PETROLIAGIS T. Error growth and estimates of predictability from the ECWMF forecasting system [J]. Quart. J. Roy. Meteor. Soc., 1995, 121: 1739-1771.

[3] FROUDE L S R, BENGTSSON L, HODGES K I. The predictability of extratropical storm tracks and the sensitivity of their prediction to the observing system [J]. Mon. Wea. Rev., 2007, 135: 315-333.

[4] FRANKLIN J L, DEMARIA M. The impact of Omega dropwindsonde observations on barotropic hurricane track forecasts [J]. Mon. Wea. Rev., 1992, 120: 381-391.

[5] ABERSON S D. Targeted observations to improve operational tropical cyclone track forecast guidance [J]. Mon. Wea. Rev., 2003, 131: 1613-1628.

[6] SNYDER C. Summary of an informal workshop on adaptive observations and FASTEX [J]. Bull. Amer. Meteor. Soc., 1996, 77: 953-961.

[7] JOLY A, JORGENSEN D, SHAPIRO M A, et al. The Fronts and Atlantic Storm-Track Experiments (FASTEX): Scientific objectives and experimental design [J]. Bull. Amer. Meteor. Soc., 1997, 78: 1917-1940.

[8] PALMER T N, GELARO R, BARKMEIJER J, et al. Singular vectors, metrics, and adaptive observations [J]. J. Atmos. Sci., 1998, 55: 633-653.

[9] ANCELL B C, MASS C F. Structure, growth rates, and tangent linear accuracy of adjoint sensitivities with respect to horizontal and vertical resolution [J]. Mon. Wea. Rev., 2006, 134: 2971-2988.

[10] WU C C, CHEN J H, LIN P H, et al. Targeted observations of tropical cyclone movement based on the Adjoint-Derived Sensitivity Steering Vector [J]. J. Atmos. Sci., 2007, 64: 2611-2626.

[11] KIM H M, MORGAN M C, MORSS R E. Evolution of analysis error and adjoint-based sensitivities: Implications for adaptive observations [J]. J. Atmos. Sci., 2004, 61: 795-812.

[12] BISHOP C H, TOTH Z. Ensemble transformation and adaptive observations [J]. J. Atmos. Sci., 1999, 56: 1748-1765.

[13] HAMILL T M, SNYDER C. Using improved background-error covariance from an ensemble Kalman filter for adaptive observations [J]. Mon. Wea. Rev., 2002, 130: 1552-1572.

[14] BISHOP C H, ETHERTON B J, MAJUMDAR S J. Adaptive sampling with the ensemble transform Kalman filter. Part I: Theoretical aspects [J]. Mon. Wea. Rev., 2001, 129: 420-436.

[15] PU Z X, KALNAY E, SELA J, et al. Sensitivity of forecast errors to initial conditions with a quasi-inverse linear method [J]. Mon. Wea. Rev., 1997, 125: 2479-2503.

[16] LORENZ E N, EMANUEL K A. Optimal sites for supplementary weather observations: Simulation with a small model [J]. J. Atmos. Sci., 1998, 55: 399-414.

[17] MU M, ZHOU F F, WANG H L. A method to identify the sensitive areas in targeting for tropical cyclone prediction: conditional nonlinear optimal perturbation [J]. Mon. Wea. Rev., 2009, 137: 1623-1639.

[18] ZHOU Fei-fan. The application of conditional nonlinear optimal perturbation to typhoon targeted observations (in Chinese) [D]. Beijing: Graduate School of Chinese Academy of Sciences. 2009: 105-115.

[19] EHRENDORFER M, ERRICO R M. Mesoscale predictability and the spectrum of optimal perturbations [J]. J. Atmos. Sci., 1995, 52: 3475-3500.

[20] DUDHIA J. A nonhydrostatic version of the Penn State /NCAR mesoscale model: Validation tests and simulation of an Atlantic cyclone and cold front [J]. Mon. Wea. Rev., 1993, 121: 1493-1513.

Citation: GAO Shou-ting, ZHOU Fei-fan and LIU Li-ping. Instability of symmetric typhoon circulation and adaptive observation. *J. Trop. Meteor.*, 2009, 15(2): 162-166.